Hindawi
Journal of Sensors
Volume 2023, Article ID 9801916, 1 page
https://doi.org/10.1155/2023/9801916

Retraction

Retracted: Recognition of Hand Gesture Using Electromyography Signal: Human-Robot Interaction

Journal of Sensors

Received 19 December 2023; Accepted 19 December 2023; Published 20 December 2023

This article has been retracted by Hindawi following an investigation undertaken by the publisher [1]. This investigation has uncovered evidence of one or more of the following indicators of systematic manipulation of the publication process:

(1) Discrepancies in scope
(2) Discrepancies in the description of the research reported
(3) Discrepancies between the availability of data and the research described
(4) Inappropriate citations
(5) Incoherent, meaningless and/or irrelevant content included in the article
(6) Manipulated or compromised peer review

The presence of these indicators undermines our confidence in the integrity of the article's content and we cannot, therefore, vouch for its reliability. Please note that this notice is intended solely to alert readers that the content of this article is unreliable. We have not investigated whether authors were aware of or involved in the systematic manipulation of the publication process.

Wiley and Hindawi regrets that the usual quality checks did not identify these issues before publication and have since put additional measures in place to safeguard research integrity.

We wish to credit our own Research Integrity and Research Publishing teams and anonymous and named external researchers and research integrity experts for contributing to this investigation.

The corresponding author, as the representative of all authors, has been given the opportunity to register their agreement or disagreement to this retraction. We have kept a record of any response received.

References

[1] S. L. Aarthy, V. Malathi, M. Hamdi, I. Hilali-Jaghdam, S. Abdel-Khalek, and R. F. Mansour, "Recognition of Hand Gesture Using Electromyography Signal: Human-Robot Interaction," *Journal of Sensors*, vol. 2022, Article ID 4718684, 9 pages, 2022.

Hindawi
Journal of Sensors
Volume 2022, Article ID 4718684, 9 pages
https://doi.org/10.1155/2022/4718684

Research Article

Recognition of Hand Gesture Using Electromyography Signal: Human-Robot Interaction

S. L. Aarthy,[1] V. Malathi,[2] Monia Hamdi,[3] Inès Hilali-Jaghdam,[4] Sayed Abdel-Khalek,[5,6] and Romany F. Mansour[7]

[1]*School of Computer Science and Engineering, Vellore Institute of Technology, Vellore, Tamil Nadu, India*
[2]*Panimalar Institute of Technology, Chennai, India*
[3]*Department of Information Technology, College of Computer and Information Sciences, Princess Nourah bint Abdulrahman University, P.O.Box 84428, Riyadh 11671, Saudi Arabia*
[4]*Department of Computer Sciences and Information Technology, Applied College, Princess Nourah Bint, Abdulrahman University, Riyadh, Saudi Arabia*
[5]*Department of Mathematics, College of Science, Taif University, P.O. Box 11099, Taif 21944, Saudi Arabia*
[6]*Department of Mathematics, Faculty of Science, Sohag University, Sohag 82524, Egypt*
[7]*Department of Mathematics, Faculty of Science, New Valley University, El-Kharga 72511, Egypt*

Correspondence should be addressed to Romany F. Mansour; romanyf@sci.nvu.edu.eg

Received 11 March 2022; Revised 29 April 2022; Accepted 30 May 2022; Published 11 July 2022

Academic Editor: Pradeep Kumar Singh

Recognition of hand gestures has been developed in various research domains and proven to have significant benefits in improving the necessity of human-robot interaction (HRI). The introduction of intelligent statistics knowledge methodologies, such as big data and machine learning, has ushered in a new era of data science and made it easier to classify hand motions accurately using electromyography (EMG) signals. However, the collecting and labelling of the vast dataset enforces a significant workload; resulting in implementations takes a long time. As a result, a unique strategy for combining the advantages of depth vision learning with EMG-based hand gesture detection was developed. It is accomplished of automatically categorizing the class of the obtained EMG data using ensemble learning without considering the hand motion sequence. The models were built and interpreted using the SVM with RBF kernel, Random Forest, and Catboost with the best hyperparameters. The resultant value states that Catboost produces the best accuracy of around 0.95 as compared with other models. This demonstrates that the suggested technique can recognize hand gestures with better performance rate.

1. Introduction

In daily existence, hand motions are viewed as a huge correspondence channel for data stream. Hand motion acknowledgment is the procedure of ordering critical hand developments. Motion association is a notable method that can be applied to a wide scope of utilizations [1, 2], including communication through signing interpretation [3], sports [4], human-robot interaction (HRI) [5, 6], and all the more comprehensively in human-machine interaction (HMI). Hand motion acknowledgment frameworks are additionally utilized in clinical applications, where bioelectrical signals are utilized rather than vision to distinguish motions. Electromyography is the most usually utilized biomedical sign for hand motion recognition and the plan of prosthetic hand regulators [7, 8]. The electrical sign delivered by solid withdrawal is estimated by EMG. The engine neuron activity possibilities produced during muscle withdrawal are the wellspring of the sign. EMG can be detected straightforwardly with cathodes set in muscle tissue or in a roundabout way with surface terminals situated over the skin [surface EMG (sEMG), which alludes to as EMG for convenience]. The EMG is more famous because of its usability and absence of intrusiveness. In the skeletal muscles, there are

a variety of physiological processes that take place. Underpin their creations, using EMG to discern between hand gestures is a difficult endeavor.

Utilizing a multimodal technique, which joins EMG with information from different sensors, is one method for avoiding these limitations. The very much acknowledged idea that specific regular cycles and peculiarities are communicated under profoundly different actual pretenses prompts multisensor information combination [9]. Multisensor frameworks, then again, further develop exactness by joining different sensors that evaluate similar sign in different however freeways. An overt repetitiveness gain limits how much vulnerability in the created data, bringing about superior precision. Late examination shows a developing interest in multitactile combination in an assortment of regions, including formative advanced mechanics [10, 11], general media signal handling, spatial discernment, consideration driven determination, and mind usefulness [12].

We take a gander at a reciprocal framework that remembers a vision sensor and EMG readings for this work. Utilizing EMG or camera frameworks has a few limitations; however, joining them offers a few advantages. For instance, EMG-based order can aid the occasion of camera obstacles, while vision characterization gives an outright estimation of finger state. For example, further developing control execution in transradial prosthetics [13] or zeroing in on perceiving objects during getting a handle on to change developments. Convolutional neural networks (CNNs) can be utilized as component separators in this last assignment [14–17]. While different info modalities further develop precision and versatility, they likewise raise registering costs because of how much information created to examine continuously, which could disturb correspondence between the individual and the prosthetic hand. Neuromorphic innovation gives an answer for these cutoff points by permitting many contributions to be handled in equal progressively while utilizing next to no power. Neuromorphic frameworks are circuits in light of natural sensory system rules that interact data using energy-productive, offbeat, occasion-driven approaches, equivalent to their organic partners. These frameworks are every now and again outfitted with web-based learning capacities that empower them to adjust to an assortment of information sources and conditions. For displaying cortical circuits, numerous neuromorphic processing frameworks have been created before, and the number is persistently extending [18, 19].

On the hand-signal acknowledgment task, the article exhibited a CNN that outflanked a support vector machine (SVM) as far as precision. The Myo armband, which distinguishes electrical movement in the lower arm muscles, was utilized to gather EMG information. From that point onward, the information was changed into spikes, which were then provided into the neuromorphic gadgets. In this paper, we present an application that outlines neuromorphic execution as far as exactness is an exhibition marker for energy utilization that is appropriate for most current processor stages and is characterized as the normal energy utilization duplicated by the normal deduction time. The period between the finish of the improvement and the arrangement is known as the surmising time. We are comparing the electromyography (EMG) signals, which gathers electrical activity from muscles using transducers created. The classification of the signals is processed using SVM with RBF kernel, Random Forest, and Catboost with the best hyperparameters.

The organization of this work is arranged in the following manner. The motivation and related works are detailed in Section 2. The framework and approaches are presented in Section 3. Section 4 describes the developed system. Section 5 depicts an experimental demonstration in a lab setup scenario. In addition, Section 6 contains findings and recommendations for further work.

2. Materials and Methods

2.1. Data Acquisition. The dataset contains around 11 k instances, each of which corresponds to a measurement collected through a medical diagnostic method called electromyography (EMG), which gathers electrical activity from muscles using transducers. The current dataset contains measurements for four different classes, with 0 denoting rock, 1 denoting scissors, 2 denoting paper, and 3 denoting okay, as illustrated in Figure 1. There are four files with 65 columns each, the first 64 of which correspond to the measurement of eight transducers from the EMG, and the last of which is the instance's class. It has a variety of cases, but the proportions are balanced. The dataset was present in the Kaggle repository (https://www.kaggle.com/georgesaavedra/hand-gestures-prediction/data).Figure 2 illustrates the sample electromyography data input. Figure 3 illustrates data visualization of the dataset which contain 11678 instances and 65 columns, with 4 different classes where 0: rock, 1: scissors, 2: paper, and 3: ok. Table 1 denotes the datasets and Table 2 represents the comparison of existing algorithm with proposed work.

2.2. Modelling

2.2.1. SVC with RBF Kernel. Due to its likeness to the Gaussian appropriation, RBF parts are nonexclusive type of kernelization and quite possibly the broadly utilized portion. For 2 focuses Y1 and Y2, the RBF part work registers their similitude, or that they are so close to another [29]. This piece can be communicated numerically as follows.

In SVC, the radial basis function is a regularly used kernel:

$$K\left(Y, Y'\right) = \exp\left(\frac{\left\|Y - Y1^{''}\right\|}{2\sigma^2}\right). \tag{1}$$

σ represets the varaince, and $\|Y - Y1^{''}\|$ is the euclidean distance between two points, Y and Y1. RBF contains two parameters namely gamma and C.

(1) Gamma

Gamma is an RBF kernel parameter; when gamma is low, the curve of choice boundary is very low, resulting in a relatively broad decision zone. When gamma is high, the decision boundary's curve is high [30].

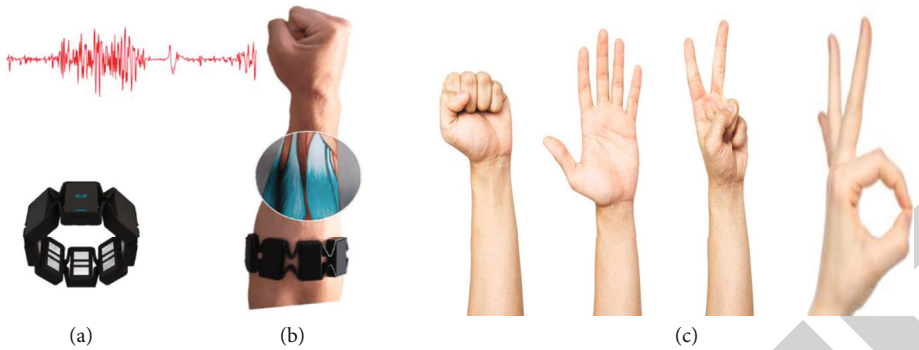

(a) (b) (c)

Figure 1: Myo armband: (a) Myo and EMG signal, (b) muscle activities on the forearm, and (c) gesture.

	0	1	2	3	4	5	6	7	8	9	...	55	56	57	58	59	60
0	26.0	4.0	5.0	8.0	−1.0	−13.0	−109.0	−66.0	−9.0	2.0	...	−28.0	61.0	4.0	8.0	5.0	4.0
1	−47.0	−6.0	−5.0	−7.0	13.0	−1.0	35.0	−10.0	10.0	−4.0	...	−25.0	47.0	6.0	6.0	5.0	13.0
2	−19.0	−8.0	−8.0	−8.0	−21.0	−6.0	−79.0	12.0	0.0	5.0	...	−83.0	7.0	7.0	1.0	−8.0	7.0
3	2.0	3.0	0.0	2.0	0.0	22.0	106.0	−14.0	−16.0	−2.0	...	−38.0	−11.0	4.0	7.0	11.0	33.0
4	6.0	0.0	0.0	−2.0	−14.0	10.0	−51.0	5.0	7.0	0.0	...	38.0	−35.0	−8.0	2.0	6.0	−13.0

Figure 2: Sample input.

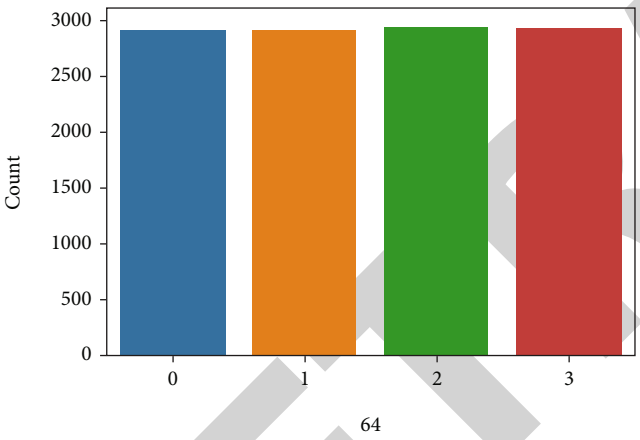

Figure 3: Dataset visualization.

Table 1: Dataset comparison.

Reference	Dataset	Total instance
[20]	Kinect gesture	6244
[21]	CGD	50,000
[22]	Microsoft kinect and leap motion	1400
[23]	Creative Senz3D	1320
[24]	MSR Gesture3D	336

(2) When C is small, the classifier does not mind if data points are misclassified i.e., high bias and low variance. Because misclassified data is highly consequenced when C is big, the classifier bends over backwards to prevent any misclassified data points, i.e., low bias and low variance [30].

(3) Gamma. Apply the same SVC-RBF classifier to the identical data in the four plots below while keeping C constant. The only difference between each graphic is that the gamma value will be increased each time. The effect of gamma can be seen on the decision boundary [30–32].

In SVM algorithm, choosing the good kernel function is much more difficult. In case if the dataset is larger, then it takes a long time.

2.2.2. Random Forest. At training, Random Forests (RFs) create a large number of individual decision trees. Ensemble approaches are named for the fact that they cause a conclusion based on a group of results. The variance decreases as the count of base learners (k) increases. Variance grows as k is reduced. However, bias remains constant throughout the procedure. Cross-validation can be used to find k [33]. The fundamental limit of Random Forest is that countless trees can make the calculation excessively sluggish and incapable of prediction. As a rule, these calculations are quick to train, however very delayed to make expectations whenever they are trained.

The basic learner should have a low bias and a high variance. As result, DT should be trained to the entire depth length. Steps involved in implementing Random Forest are illustrated below:

Step 1: Consider the training informational collection has N perceptions and M elements. To start, an arbitrary example from the training informational collection is taken with substitution

Step 2: A subset of M qualities is picked indiscriminately, and the best parted include is used to part the hub recursively

Step 3: The tree has arrived at its regular

Step 4: The previous stages are rehashed, and a conjecture is made in light of the number of expectations from n trees

The training time, run time, and space complexity are as follows: Training time = $O(\log(nd) * L)$, Run time = $O(dp$

Table 2: Comparison of hand gesture recognition system.

Reference	Dataset	Count of the gesture data	Techniques utilized	Resultant analysis
[25]	Own dataset	60	Block scaling	84%
[26]	American sign language (ASL)	208	Neural networks	92.78%
[27]	Arabic numbers	298	BP neural network	90.45%
[28]	Own dataset	130	Self-growing and self-organizing neural gas	90.45%

For b = 1 to B:
For a = 1 to A:
(a) Inducement a boostrap model Z*, which of the size N derived from training samples
(b) Develop a RFT Tr_b to the bootstrapped information, by recursively rehashing the subsequent phases for every terminal hub of the tree, till the smallest node scope n_{min} is collected
1) choose the m variables at arbitrary
2) select the finest variables
3) Divide the nodes into 2 sub nodes
2. Produce the ensemble tree $\{Tb\}$A.
To make an expectation at another point x:
Regression: $M_{rf}^{a}(y) = 1/a\sum_{a=1}^{A} Tb(y)$.
Classification: Wb(x) be the class expectation of the RFT, it cab be written as,
$W_{rf}^{A}(x) = majority\ vote\ \{c_b(x)\}^{A}$.

Algorithm 1: Random Forest for classification

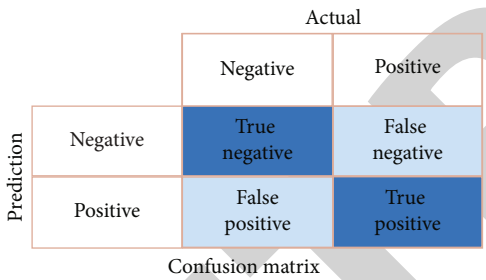

Figure 4: Confusion matrix.

Table 3: Performance evaluation metrics of SVC with RBF kernel.

Classes	Precision	Recall	F1 score	Support
0	0.93	0.97	0.95	417
1	0.92	0.96	0.94	426
2	0.95	0.91	0.93	472
3	0.90	0.86	0.88	437
Accuracy			0.93	1752
Macro avg	0.92	0.93	0.93	1752
Weighted avg	0.93	0.93	0.92	1752

∗ L), and Space = O(MT ∗ L). As the count of base models grows, the training run time grows; hence, cross-validation is always used to discover the best hyperparameter.

2.2.3. Catboost. Yandex's team created Catboost, an open-source gradient boosting technique, in 2017. It is a machine learning technique that distinguishes itself from XGBoost and LightGBM by allowing users to easily handle categorical features for a big dataset. Catboost can be used to tackle problems including regression, classification, and ranking. The benefits of Catboost algorithm is that it is supposed to be quicker in execution of GPU/CPU training and the model quality improved and the overfitting problem is avoided.

Catboost can give lists to unmitigated sections, taking into consideration one-hot encoding utilizing one-hot max size (use one-hot encoding for all highlights with number of various qualities not exactly or equivalent to the given boundary esteem) [34–38].

$$Average_{target} = \frac{Countinclass + Prior}{total\ count + 1}, \tag{2}$$

where CountInClass is the number of times the label value for objects with the current straight out highlight esteem was equal to "1."

The numerator's preliminary value is called prior. The beginning settings decide this. The entire count of substances with an unconditional feature rate that matches the existing one is called TotalCount. Numerically, this can be addressed utilizing beneath condition:

$$\frac{\sum_{k=1}^{q-1}\left[y\sigma_k = y_{\sigma\, q,k}\right] W_{\sigma k} + b.q}{\sum_{k=1}^{q-1}\left[y\sigma_k = y_{\sigma\, q,k}\right] W_{\sigma k} + b}. \tag{3}$$

Catboost adopts well for distributed computing; it produces higher training accuracy as compared with Random Forest. Catboost algorithm reduces the overfitting problem.

2.3. System Configuration. The experiment was implemented in the following hardware: Intel(R) Core(TM) i5-8300H

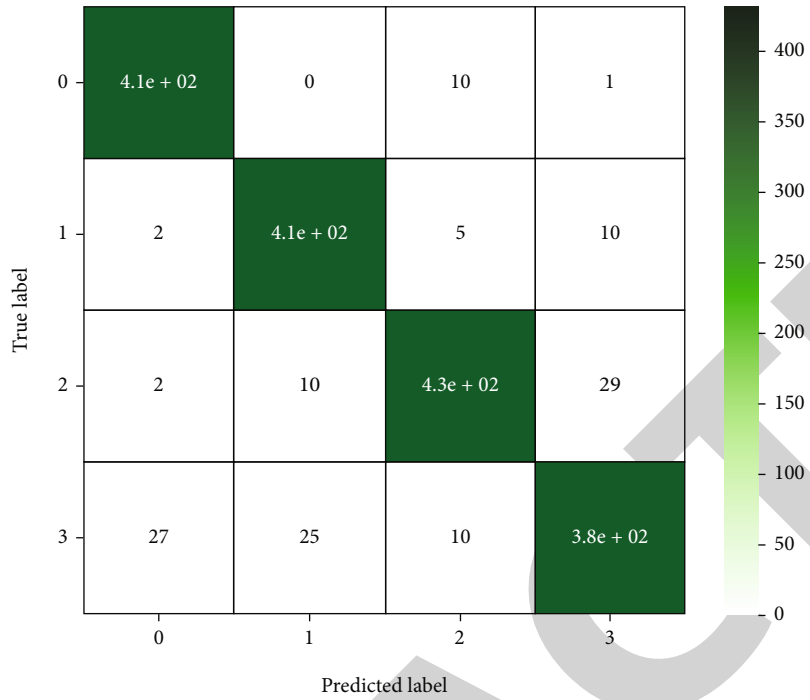

Figure 5: Confusion matrix of SVC with RBF kernel.

Table 4: Performance evaluation metrics of Random Forest.

Classes	Precision	Recall	F1 score	Support
0	0.91	0.99	0.95	417
1	0.96	0.92	0.94	426
2	0.91	0.95	0.93	472
3	0.93	0.85	0.89	437
Accuracy			0.93	1752
Macro avg	0.93	0.93	0.93	1752
Weighted avg	0.93	0.93	0.93	1752

CPU @ 2.30 GHz, 8GB RAM, 64-bit Operating System, ×64 based processor, GPU NVIDIA GTX1050 with 4G memory and software specification, Anaconda navigator tool, and Python programming.

3. Results and Discussions

3.1. Performance Evaluation Metrics. The term accuracy usually implies classification accuracy. The quantity of right expectations partitioned by the all out number of info tests is the proportion. It possibly works when there are an equivalent number of tests in each class. At the argument whenever a comparable model is surveyed on a test set with 60% class A examples and 40% class B tests, the test exactness drops to 60%. At the point when the expense of misclassification of minor class tests is extremely enormous, the main problem shows up. The confusion matrix creates a framework as a result, which portrays the model's general presentation. Precision, recall, and F1 score are the assessment measures used to assess the model's concert as illustrated in Figure 4. When dealing with erratic data, accuracy performance measures are crucial [35, 39–44].

Precision states what percentage of all the optimistic predictions is genuinely positive:

$$precision = \frac{True\ positive}{True\ positive + False\ positive}. \tag{4}$$

Recall states what extent of the all out certain is expected to be positive:

$$Recall = \frac{True\ positive}{True\ positive + False\ positive}. \tag{5}$$

A harmonic mean exists between precision and recall. It receipts mutually false positives and false negatives taken into consideration. As a result, it achieves fine with a dataset that is unbalanced.

$$\text{F1 score} = 2 * \frac{Precision * Recall}{Precision + Recall}. \tag{6}$$

Recall and precision are given equal weighting in the F1 score.

There is a weighted F1 score that allows us to assign different weights to recall and precision. Recall and precision are assigned different weights in different issues, as described in the previous section:

$$F_\beta = \left(1 + \beta^2\right) * \frac{\text{Precision} * \text{Recall}}{\left(\beta^2 * \text{Precision}\right) + \text{Recall}}. \tag{7}$$

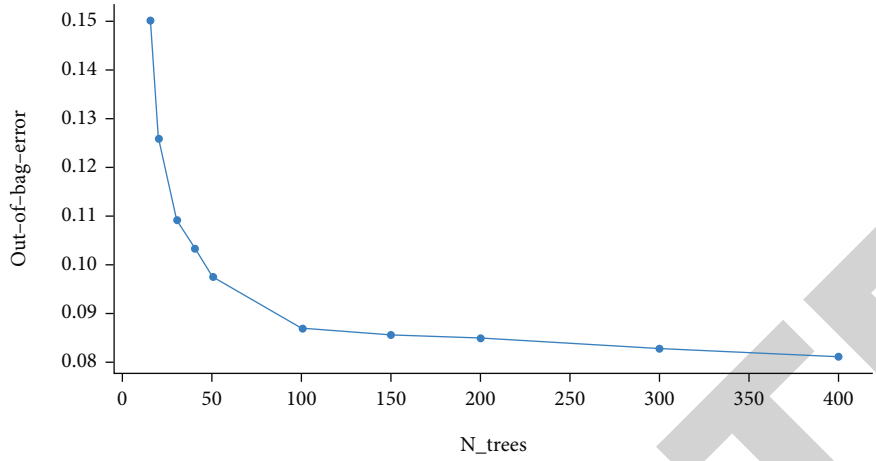

Figure 6: Out of bag error with respect to n_trees.

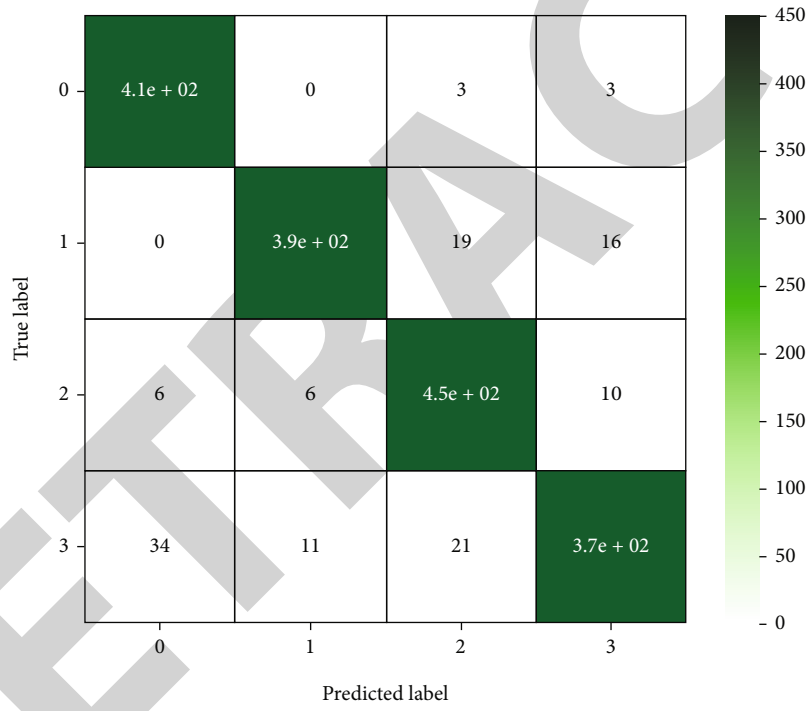

Figure 7: Confusion matrix of Random Forest.

Table 5: Performance evaluation metrics of Catboost classifier.

Classes	Precision	Recall	F1 score	Support
0	0.97	0.97	0.97	417
1	0.98	0.96	0.97	426
2	0.94	0.95	0.94	472
3	0.94	0.93	0.94	437
Accuracy			0.95	1752
Macro avg	0.95	0.95	0.95	1752
Weighted avg	0.95	0.95	0.95	1752

Beta is the number of times higher priority than accuracy. Assuming that the review is two times as significant as accuracy, the worth of beta is 2.

3.1.1. SVC with RBF Kernel. Table 3 illustrates the performance evaluation metrics for the DVC with RBF kernel. The performance of the model was calculated using the evaluation metrics namely precision, recall, F1 score, and support. It was observed that the precision value was more for the class 2 0.95, recall value was higher for the class 1 0.97, and F1 score was higher for the class 1 0.95. Confusion matrix is illustrated in Figure 5.

3.1.2. Random Forest. Table 4 illustrates the performance evaluation metrics for the Random Forest. The performance of the model was calculated using the evaluation metrics namely precision, recall, F1 score, and support. It was observed that the precision value was more for the class 1 around 0.96, recall value was higher for the class 2 around

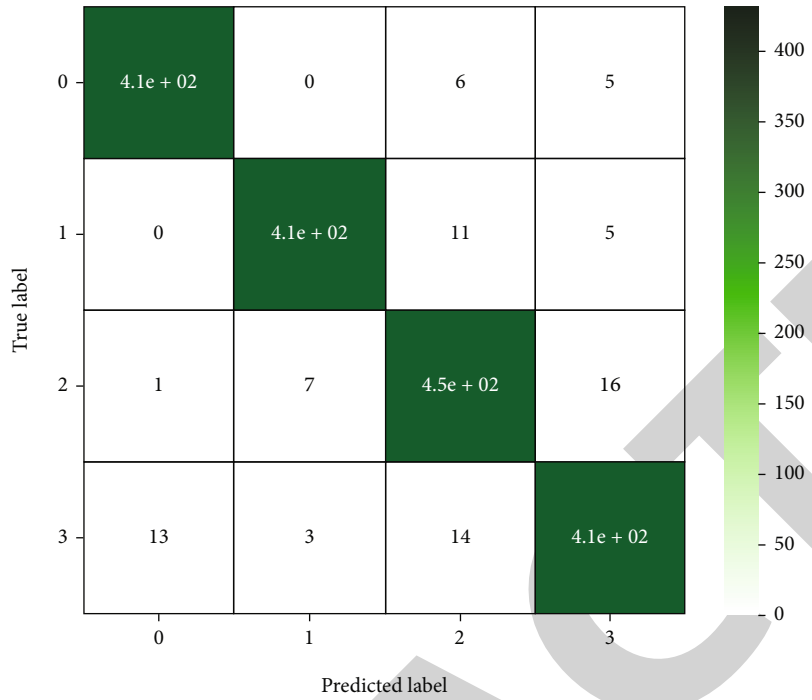

Figure 8: Confusion matrix of Catboost classifier.

Table 6: Hyperparameters of classification algorithm.

Methods	Hyperparameters
SVC	Kernel = "rbf," c = 15, gamma = 0.01, decision_function_shape = "ovc," probability = true
Random Forest	Random_state = 42, warm_state = true, n_jobs = −1, obb_score = true
Catboost	Iteration = 300, learning_rate = 0.7, random_seed = 42, depth = 5

Table 7: Interpretation of classification algorithms.

Metrics	Support vector classifier	Random Forest	Catboost
Precision	0.925	0.927	0.953
Recall	0.925	0.926	0.953
Fscore	0.924	0.925	0.953
Accuracy	0.925	0.926	0.953
Auc	0.950	0.950	0.968

0.95, and F1 score was higher for the class 1 around 0.95. Confusion matrix was illustrated in the table. The resultant value states that Random Forest performs well as compared with SVC with kernel. Figure 6 illustrated the Out of bag error with respect to n_trees. The confusion matrix of Random Forest is illustrated in Figure 7.

3.1.3. Catboost Classifier. Table 5 illustrates the performance evaluation metrics for the Catboost classifier. The performance of the model was calculated using the evaluation metrics namely precision, recall, F1 score, and support. It was observed that the precision value was more for the class 2 around 0.98, recall value was higher for the class 1 around 0.97, and F1 score was higher for the class 1 around 0.97. The overall accuracy was achieved around 0.95, macro average was 0.95, and weighted average was 0.95. The confusion matrix is illustrated in Figure 8. Table 6 illustrates the hyperparameters of classification algorithm. Table 7 illustrates the interpretation of classification algorithms based on the following metrics namely precision, recall, F1 score, and support. The resultant value states that the Catboost algorithm performs better as compared with the SVC and Random forest.

4. Conclusion and Future Work

The proposed work classifies various hand motions using EMG signals. Any human computer focused systems or gadgets can be controlled using the signal. The results of the experiment reveal that the Catboost classifier–based NN distinguishes the necessary signals quickly and efficiently. The developed model was found to successfully classify EMG signals based on hand gestures with a typical accuracy amount of 9.31 percent. If the network is fed additional evocative EMG inputs, classification efficiency can be improved. The EMG signals, on the other hand, differ every now and again and from subject to subject. The cat boost classifier has been found to recognize the desired motions efficiently and with

computational cost. The developed model correctly identified the gestures in a short amount of time. The EMG signals that have been categorized utilized to create a human mainframe interface that allows disabled people to interact with computers. The integration of muCI with human-robot interaction applications will be the focus of future effort. A basic learning method is also used to explain the muCI. We planned to use augmented reality to combine hand gesture detection with surgical robot control and training. IoT-based sensor can be incorporated in the future. Other sophisticated learning approaches, such as deep learning, will be used in future research.

Data Availability

The dataset was present in the Kaggle repository (https://www.kaggle.com/georgesaavedra/hand-gestures-prediction/data).

Conflicts of Interest

There is no conflict of interest.

Acknowledgments

This research was funded by Princess Nourah bint Abdulrahman University Researchers Supporting Project number (PNURSP2022R125), Princess Nourah bint Abdulrahman University, Riyadh, Saudi Arabia.

References

[1] E. Ceolini, C. Frenkel, S. B. Shrestha et al., "Hand-gesture recognition based on EMG and event-based camera sensor fusion: a benchmark in neuromorphic computing," *Frontiers in Neuroscience*, vol. 14, p. 637, 2020.

[2] M. Yasen and S. Jusoh, "A systematic review on hand gesture recognition techniques, challenges and applications," *PeerJ Computer Science*, vol. 5, article e218, 2019.

[3] M. J. Cheok, Z. Omar, and M. H. Jaward, "A review of hand gesture and sign language recognition techniques," *International Journal of Machine Learning and Cybernetics*, vol. 10, no. 1, pp. 131–153, 2019.

[4] J. F. Loss, D. Cantergi, F. M. Krumholz, M. La Torre, and C. T. Candotti, "Evaluating the electromyographical signal during symmetrical load lifting," in *Applications of EMG in Clinical and Sports Medicine, ed C*, p. 1, Books on Demand, Steele, Norderstedt, 2012.

[5] G. Cicirelli, C. Attolico, C. Guaragnella, and T. D'Orazio, "A kinect-based gesture recognition approach for a natural human robot interface," *International Journal of Advanced Robotic Systems*, vol. 12, no. 3, p. 22, 2015.

[6] H. Liu and L. Wang, "Gesture recognition for human-robot collaboration: a review," *International Journal of Industrial Ergonomics*, vol. 68, pp. 355–367, 2018.

[7] S. Benatti, F. Casamassima, B. Milosevic et al., "A versatile embedded platform for EMG acquisition and gesture recognition," *IEEE Transactions on Biomedical Circuits and Systems*, vol. 9, no. 5, pp. 620–630, 2015.

[8] E. Donati, M. Payvand, N. Risi, R. B. Krause, and G. Indiveri, "Discrimination of EMG signals using a neuromorphic implementation of a spiking neural network," *IEEE Transactions on Biomedical Circuits and Systems*, vol. 13, no. 5, pp. 795–803, 2019.

[9] D. Lahat, T. Adali, and C. Jutten, "Multimodal data fusion: an overview of methods, challenges, and prospects," *Proceedings of the IEEE*, vol. 103, no. 9, pp. 1449–1477, 2015.

[10] A. Droniou, S. Ivaldi, and O. Sigaud, "Deep unsupervised network for multimodal perception, representation and classification," *Robotics and Autonomous Systems*, vol. 71, pp. 83–98, 2015.

[11] O. Zahra and D. Navarro-Alarcon, "A self-organizing network with varying density structure for characterizing sensorimotor transformations in robotic systems," in *Towards Autonomous Robotic Systems*, K. Althoefer, J. Konstantinova, and K. Zhang, Eds., pp. 167–178, Springer International Publishing, Cham, 2019.

[12] S. Braun, D. Neil, J. Anumula, E. Ceolini, and S. Liu, "Attention driven multi-sensor selection," in *2019 International Joint Conference on Neural Networks (IJCNN)*, pp. 1–8, Budapest, Hungary, 2019.

[13] M. Markovic, S. Dosen, D. Popovic, B. Graimann, and D. Farina, "Sensor fusion and computer vision for context-aware control of a multi degree-of-freedom prosthesis," *Journal of Neural Engineering*, vol. 12, no. 6, article 066022, 2015.

[14] V. Malathi and M. P. Gopinath, "Classification of pest detection in paddy crop based on transfer learning approach," *Science*, vol. 71, no. 7, pp. 552–559, 2021.

[15] V. Malathi and M. P. Gopinath, "A review on rice crop disease classification using computational approach," *International Journal of Image and Graphics*, vol. 2240007, 2021.

[16] V. Malathi and M. P. Gopinath, "Noise deduction in novel paddy data repository using filtering techniques," *Scalable Computing: Practice and Experience*, vol. 21, no. 4, pp. 601–610, 2020.

[17] V. Malathi and M. P. Gopinath, "Classification of diseases in paddy using deep convolutional neural network," *Journal of Physics: Conference Series*, vol. 1964, no. 4, article 042028, 2021.

[18] N. Qiao, H. Mostafa, F. Corradi et al., "A reconfigurable on-line learning spiking neuromorphic processor comprising 256 neurons and 128k synapses," *Frontiers in Neuroscience*, vol. 9, p. 141, 2015.

[19] S. Moradi, N. Qiao, F. Stefanini, and G. Indiveri, "A scalable multicore architecture with heterogeneous memory structures for dynamic neuromorphic asynchronous processors (DYNAPs)," *IEEE Transactions on Biomedical Circuits and Systems*, vol. 12, no. 1, pp. 106–122, 2018.

[20] "Kinect gesture dataset," 2019, https://www.microsoft.com/en-us/download.

[21] "ChaLearn gesture dataset," 2019, http://gesture.chalearn.org/data.

[22] G. Marin, F. Dominio, and P. Zanuttigh, "Hand gesture recognition with leap motion and kinect devices," in *2014 IEEE International conference on image processing (ICIP)*, pp. 1565–1569, Paris, France, 2014.

[23] A. Memo, L. Minto, and P. Zanuttigh, *Exploiting Silhouette Descriptors and Synthetic Data for Hand Gesture Recognition*, The Eurographics Association, 2015.

[24] A. Kurakin, Z. Zhang, and Z. Liu, "A real time system for dynamic hand gesture recognition with a depth sensor," in

2012 Proceedings of the 20th European signal processing conference (EUSIPCO), pp. 1975–1979, Bucharest, Romania, 2012.

[25] M. M. Hasan and P. K. Misra, "Brightness factor matching for gesture recognition system using scaled normalization," *AIRCC's International Journal of Computer Science and Information Technology*, vol. 3, no. 2, pp. 35–46, 2011.

[26] V. S. Kulkarni and S. D. Lokhande, "Appearance based recognition of American sign language using gesture segmentation," *International Journal on Computer Science and Engineering*, vol. 2, no. 3, pp. 560–565, 2010.

[27] S. Zhao, W. Tan, S. Wen, and Y. Liu, "An improved algorithm of hand gesture recognition under intricate background," in *International Conference on Intelligent Robotics and Applications*, pp. 786–794, Springer, Berlin, Heidelberg, 2008.

[28] E. Stergiopoulou and N. Papamarkos, "Hand gesture recognition using a neural network shape fitting technique," *Engineering Applications of Artificial Intelligence*, vol. 22, no. 8, pp. 1141–1158, 2009.

[29] Z. A. A. Hammouri, M. F. Delgado, E. Cernadas, and S. Barro, "Fast SVC for large-scale classification problems," *IEEE Transactions on Pattern Analysis and Machine Intelligence*, vol. PP, p. 1, 2021.

[30] A. Muratyan, W. Cheung, S. V. Dibbo, and S. Vhaduri, "Opportunistic multi-modal user authentication for health-tracking IoT wearables," 2021, http://arxiv.org/abs/2109.13705.

[31] D. Koundal, "Texture-based image segmentation using neutrosophic clustering," *IET Image Processing*, vol. 11, no. 8, pp. 640–645, 2017.

[32] K. Bhalla, D. Koundal, B. Sharma, Y. C. Hu, and A. Zaguia, "A fuzzy convolutional neural network for enhancing multi-focus image fusion," *Journal of Visual Communication and Image Representation*, vol. 84, article 103485, 2022.

[33] Z. K. Senturk and M. S. Bakay, "Machine learning based hand gesture recognition via EMG data," *Advances in Distributed Computing and Artificial Intelligence Journal*, vol. 10, no. 2, 2021.

[34] N. Nahar, F. Ara, M. Neloy et al., "Feature selection Based Machine Learning to Improve Prediction of Parkinson Disease," in *International Conference on Brain Informatics*, pp. 496–508, Springer, Cham, 2021.

[35] D. Chicco, N. Tötsch, and G. Jurman, "The Matthews correlation coefficient (MCC) is more reliable than balanced accuracy, bookmaker informedness, and markedness in two-class confusion matrix evaluation," *BioData Mining*, vol. 14, no. 1, pp. 1–22, 2021.

[36] D. Koundal, S. Gupta, and S. Singh, "Neutrosophic based Nakagami total variation method for speckle suppression in thyroid ultrasound images," *IRBM*, vol. 39, no. 1, pp. 43–53, 2018.

[37] N. Salankar, D. Koundal, C. Chakraborty, and L. Garg, "Automated attention deficit classification system from multimodal physiological signals," *Multimedia Tools and Applications*, pp. 1–16, 2022.

[38] M. Zakariah, Y. A. Alotaibi, D. Koundal, Y. Guo, and M. Mamun Elahi, "Sign language recognition for Arabic alphabets using transfer learning technique," *Computational Intelligence and Neuroscience*, vol. 2022, 15 pages, 2022.

[39] S. Bhat and D. Koundal, "Multi-focus image fusion using neutrosophic based wavelet transform," *Applied Soft Computing*, vol. 106, article 107307, 2021.

[40] S. Bhat and D. Koundal, "Multi-focus image fusion techniques: a survey," *Artificial Intelligence Review*, vol. 54, no. 8, pp. 5735–5787, 2021.

[41] A. Prasad, A. K. Tyagi, M. M. Althobaiti, A. Almulihi, R. F. Mansour, and A. M. Mahmoud, "Human activity recognition using cell phone-based accelerometer and convolutional neural network," *Applied Sciences*, vol. 11, no. 24, p. 12099, 2021.

[42] S. Aggarwal, S. Gupta, A. Alhudhaif, D. Koundal, R. Gupta, and K. Polat, "Automated COVID-19 detection in chest X-ray images using fine-tuned deep learning architectures," *Expert Systems*, vol. 39, no. 3, article e12749, 2022.

[43] D. Koundal, B. Sharma, and Y. Guo, "Intuitionistic based segmentation of thyroid nodules in ultrasound images," *Computers in Biology and Medicine*, vol. 121, article 103776, 2020.

[44] M. N. Hossen, V. Panneerselvam, D. Koundal, K. Ahmed, F. M. Bui, and S. M. Ibrahim, "Federated machine learning for detection of skin diseases and enhancement of internet of medical things (IoMT) security," *IEEE Journal of Biomedical and Health Informatics*, p. 1, 2022.